Permafrost protection by thermosyphon under the paved road in West Mongolia

Jambaljav Yamkhin[1], Namdag Choibalsan[2], Tsogt-Erdene Gansukh[3] & Ulambayar Ganbold[3]

[1]*Geocryo LLC, Ulaanbaatar, Mongolia*

[2]*Newcon LLC, Ulaanbaatar, Mongolia*

[3]*Permafrost Department of Institute of Geography and Geoecology, Ulaanbaatar, Mongolia*

ABSTRACT

According to the results of field studies, asphalt pavement increases the absorption of solar radiation and the accumulation of snow or water in the channels on both sides of the road, accelerating the thawing of permafrost under it, and due to this process, waves form on the asphalt surface and driving on it at normal speed becomes dangerous. Field measurements show that the rate of permafrost thawing under natural conditions is 0.5–2.0 cm per year, and permafrost thawing under paved roads is 5–10 times faster than under natural conditions. In 2021–2022, in close cooperation with construction companies, government officers, and permafrost experts, a road with a thermosyphon embankment was built in an ice-rich permafrost area along the western road corridors at six selected road sections. On December 1, 2022, the ground temperature dropped to -14 °C and -20 °C at the evaporator, while in the ground between the thermosyphons dropped to -8 °C or -9 °C. These temperatures increased to +1.6 °C and -0.7 °C at the evaporator and to -0.9 °C and -2.2 °C between thermosyphons. In Mongolia, the thermosyphon works very well, but under the paved road above the evaporators, it is necessary to install pretty good insulation.

1 INTRODUCTION

Permafrost can be understood as a mixture of frozen ground and ice. Under natural conditions, ice contents are different along the permafrost profile. Due to climate warming, permafrost degrades differently, and it degrades faster in Mongolia because Mongolian permafrost is characterized by sensible permafrost with a temperature close to zero degrees (Sharkhuu et al. 2011; Jambaljav et al. 2013, 2017; Ishikawa et al. 2018; Yamkhin et al. 2022).

More than 1,400 km of Mongolian roads pass through the permafrost regions (Figure 1), and some parts of these roads on ice-rich permafrost are damaged.

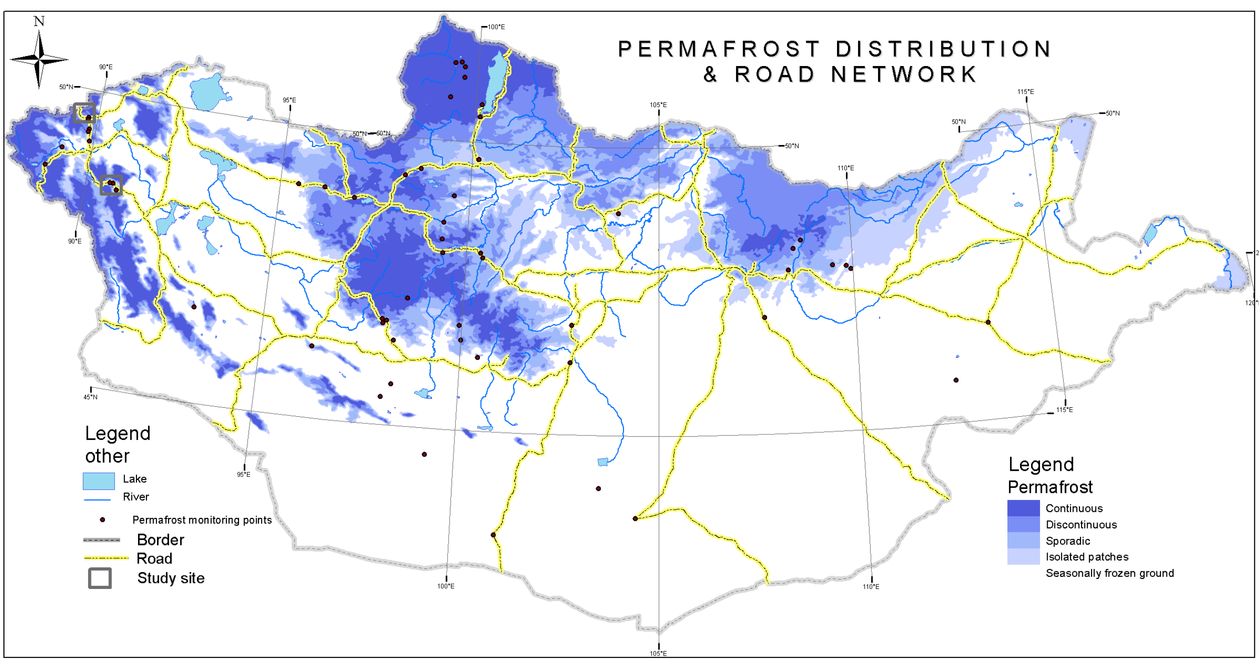

Figure 1. Permafrost distribution and road network over Mongolia.

Jambaljav et al. (2019) reported on the state of permafrost along the roads of Mongolia, and as a result of this study, permafrost degrades 5–10 times faster under a paved road compared to permafrost degradation in natural conditions.

According to the results of field studies, asphalt pavement increases the absorption of solar radiation and the accumulation of snow or water in the channels on both sides of the road, accelerating the thawing of permafrost under it, and due to this process, waves form on the asphalt surface and driving on it at normal speed becomes dangerous. Seventy-five percent of traffic accidents occur on countryside roads, and one of the reasons for these accidents is the subsidence of the road surface due to the thawing of permafrost (mrtd.gov.mn).

The permafrost temperature is requested to be cooled down under asphalt-paved roads for warm permafrost regions (Cheng et al. 2008). There are several methods of embankment bed cooling to prevent the permafrost thaw. Here we discuss permafrost studies using electrical resistivity tomography (ERT) along the road in the western regional corridor of Mongolia between Russia and China and monitoring results of ground temperature under roads with thermosyphon cooling and without thermosyphon cooling.

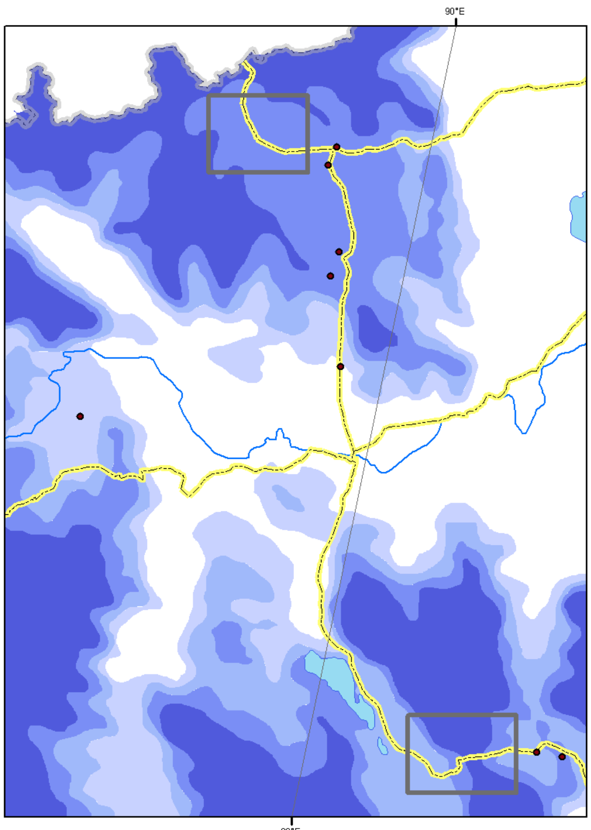

Figure 2. Location of study sites, legend is same as in Figure 1

1.1 Study sites

Our study sites are located in the far west along the western road corridor of Mongolia between Russia and China (Figure 2).

The first site is located at Buraat Pass with an elevation of 2370–2560 m asl. The second site is located between an intermountain valley with an elevation of 2280 m asl, near the Mongolian and Russian border. Both sites have permafrost from discontinuous to continuous distribution.

Cryogenic phenomena such as pingo-like mounds, thermokarst lakes, dog holes in intermountain depressions, and valleys are widely developing.

Ground materials are lacustrine sediments in intermountain depressions, and gravels with sandy fill are typical sediments in intermountain valleys and mountain food slopes. Ice contents are more than 50% along this road in some parts.

Permafrost monitoring has been carried out in boreholes near these study sites since 2009. Permafrost temperature is -0.42ºC at a depth of 10 m in borehole “Hongor-Olon", near site 1, and -0.5ºC at a depth of 10 m in borehole “Tsagaannuur-2”, near site 2. The active layer thickness increases by 0.5–2.0 cm annually (Sharkhuu et al. 2011).

In site 1, we installed inclined thermosiphons on three sections and looped thermosyphons on one section of the paved road following the formation of waves on the road surface in 2021–2022. In 2022–2023, during the construction of the road, inclined thermosyphons were installed on three sections of the paved road in site 2.

In site 1, permafrost studies were conducted after 2 years of road construction, and in site 2, permafrost studies were conducted before one year of road construction. Here, permafrost study and monitoring results are reported for site 2.

2 METHODS

ERT surveys have been conducted along or across roads to study permafrost under paved roads after and before construction. Temperature measurements under roads were made using a thermistor string and data loggers from Onset Computer Corporation.

2.1 Electrical Resistivity Tomography (ERT)

Electrical resistivity surveys have been used for many decades in hydrological, mining, and geotechnical investigations. More recently, it has been used for environmental surveys. The resistivity measurements are commonly made by injecting current into the ground through two current electrodes and measuring the resulting voltage difference at two potential electrodes (Loke 2001). The Ground resistivity is related to various geological parameters such as the mineral and fluid content, porosity, and degree of water saturation. The enormous contrast between groundwater (10–100Ωm) and underground ice (> 1000 Ωm) provides an excellent opportunity to determine frozen and unfrozen layers from the surface surveys. Here, we used the Syscal R1+ with Wenner or Wenner-

Schlumberger arrays. Our measurements were carried out along and across the road with a distance between electrodes of 1–5 m and with 48, 64, and 80 electrodes (Figure 3). Penetration depth depends on the configuration of arrays. Maximum penetration depth was 80 m.

Figure 3. ERT survey across the road, Wenner-Schlumberger array with 1 m spacing

2.2 Temperature measurements

Under paved roads, inclined holes were drilled at an angle of 30 degrees with a distance of 3 m between them, into which iron pipes with a diameter of 50 mm (thermosyphon evaporators) and a PVC tube with a diameter of 15 mm were inserted. Some 15 mm PVC tubes have thermistors and data loggers to monitor the temperature under the paved road (Figure 4).

In addition, we record the temperature under paved roads without thermosyphons to compare the cooling effects.

Figure 4. Monitoring box: temperature sensors are installed in white PVC tubes at the end of the evaporator tube and between the thermosyphons.

3 RESULTS

3.1 ERT survey results at site 2

There are three sections, 200 m long (k13+600:k13+800), 160 m long (k14+360:k14+500), and 140 m long (k15+160:k15+300), on which inclined thermosyphons with a spacing of 3 m were place on site 2 in 2022. At all three sites, surface cuts were made before the ERT survey for the next phase of road construction. Waves of thawing permafrost formed on the surface.

3.1.1 Section 1 (k13+600:k13+800)

The section has a total length of 200 m towards the Russian-Mongolian border and is located in the foothills with short vegetation covering the eastern part of the mountain range. In the excavation, subsidence is observed on the surface due to permafrost thawing along the road. Here, 4 ERT measurements were carried out, and boreholes were drilled at certain points on the electrodes of these ERT profiles. We placed one profile with a distance between electrodes of 5 m along the road and 3 more profiles with a distance between electrodes of 1 m crossed the road. The first profile has a length of 400 m and a penetration depth of > 75 m, and the remaining 3 profiles have a length of 64 m and a penetration depth of 13 m. We set the electrical resistivity value from 50 Ω*m to > 14595 Ω*m to make the profiles visible. It is visible that below the active layer, there is a layer of permafrost 12–15 m deep with a variety of ice (Figure 5).

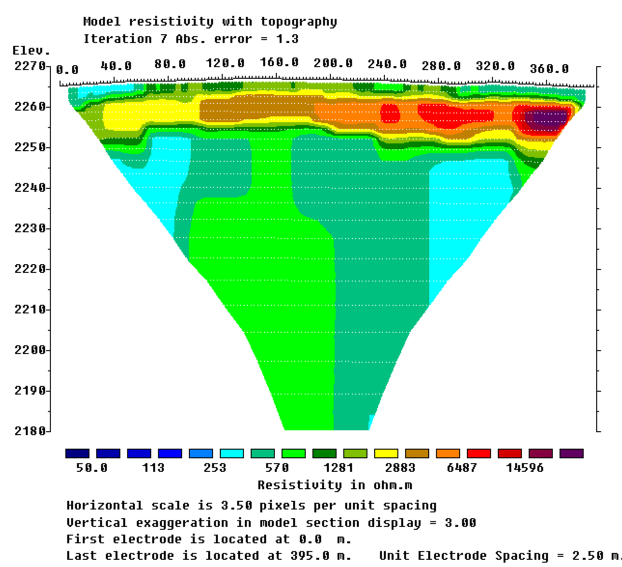

Figure 5. ERT profile along the road section k13+600:k13+800. The depth of penetration is > 75 m. The value of electrical resistivity ranged from 50Ω*m to > 14595Ω*m.

Another 3 profiles have a similar pattern of electrical resistivity images. Therefore, we provide here a description of all profiles together. The profiles received the numbers k13-2, k13-3 and k13-4. Boreholes were also drilled on electrodes No. 32 of profile k13-2, No. 32 of profile k13-3, and No. 56 of profile k13-4. Boreholes K13-2-32 and K13-3-32 are located in the center of the profiles, and borehole k13-2-56 was drilled on the side of the road, located in pristine natural conditions.

As a result of drilling boreholes, soil samples were taken for bulk density, moisture, excess ice, free settlement after thawing, and grain size. The core is dominated by gravel with yellowish sand. Soil density is 1.1–1.76 g/cm^3, moisture is 26.51–76.92%, and 0.5 cm is thaw settlement when thawing a 6 cm layer. In these boreholes and other boreholes of the site, as well as by ERT profiles, the thickness of the active layer is 2–3.1 m. It is visible that the thickness of the active layer is 2–3 m, and some permafrost thawing on both sides of the main direction of the road (Figure 6).

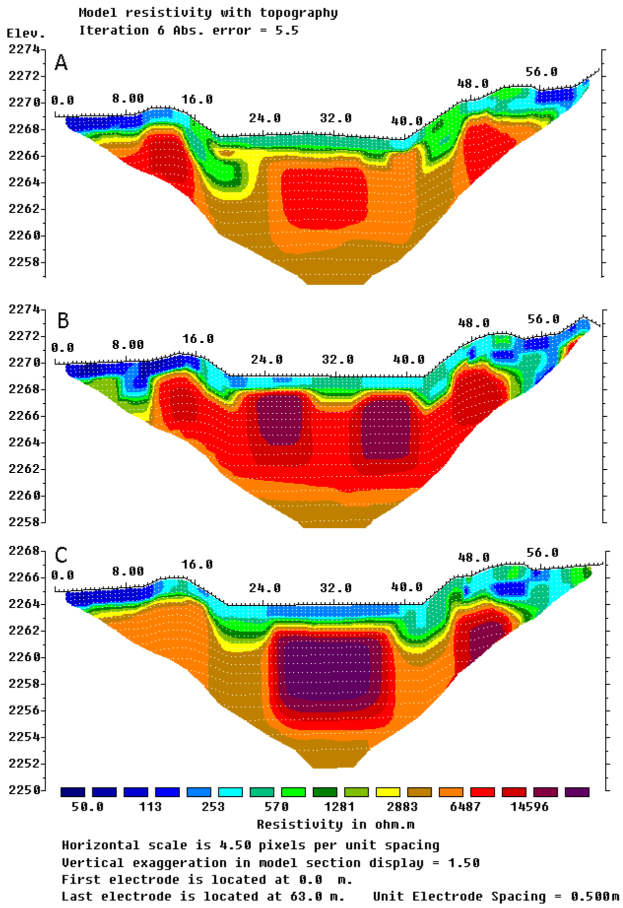

Figure 6. Transverse ERT profiles of the road in section 1 of site 2. The resistivity value is the same as in Figure 2.

3.1.2 *Section 2 (k14+360:k14+500)*

Electrical resistivity tomography profile k14-1 is located along the road, and ERT profile k14-2 is located across the excavations. The borehole was drilled on electrode no. 24 of ERT profile k14-2. The ERT profile layout and soil materials from the borehole are similar to the previous section 1 regarding soil composition, active layer thickness, and permafrost conditions. The difference is that the resistivity values are lower below the permafrost on both ERT profiles compared to section 1, and lower resistivity values appeared under the main road, but it is around 4324.88 Ω*m. We hypothesized that the lower resistivity beneath the permafrost may be due to lacustrine sediments. The main direction surface has waves and a permafrost thawing bowl on both sides of the main road (Figures 7 and 8).

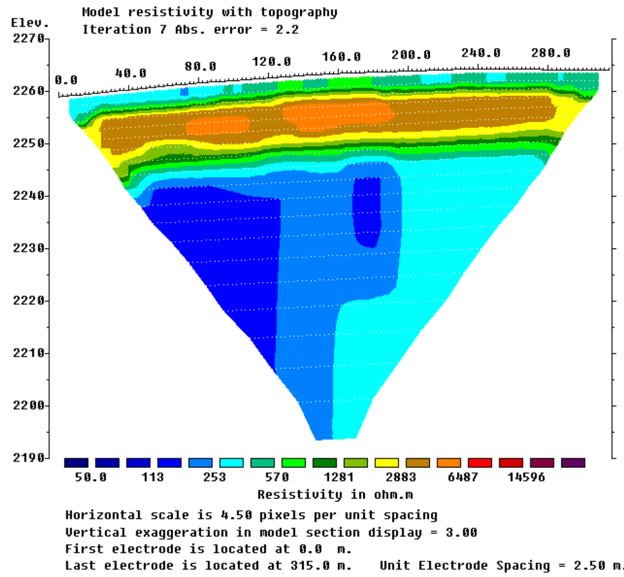

Figure 7. ERT profile along the road at section 2. The penetration depth, profile length, and resistivity value are the same as in Figure 2.

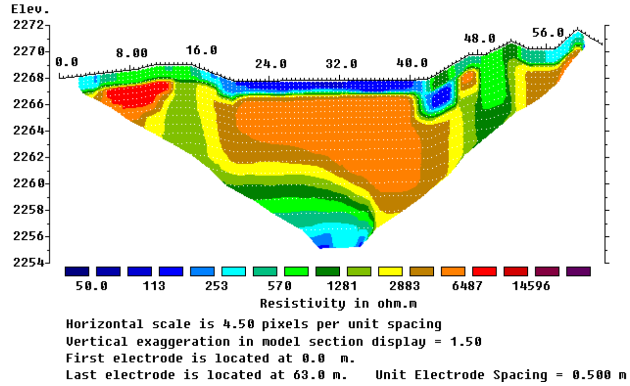

Figure 8. Transverse ERT profile of the road in section 2 of site 2. The penetration depth and resistivity value are the same as in Figure 3.

3.1.3 Section 3 (k15+160:k15+300)

There are 2 ERT profiles across the excavations (Figure 9).

The boreholes were drilled on electrode No. k15-1-36 and on electrode No. k15-2-20. Core samples and the pattern of ERT profiles are similar to section 1. The thickness of the active layer is from 2 to 3 m. Permafrost has a high ice content.

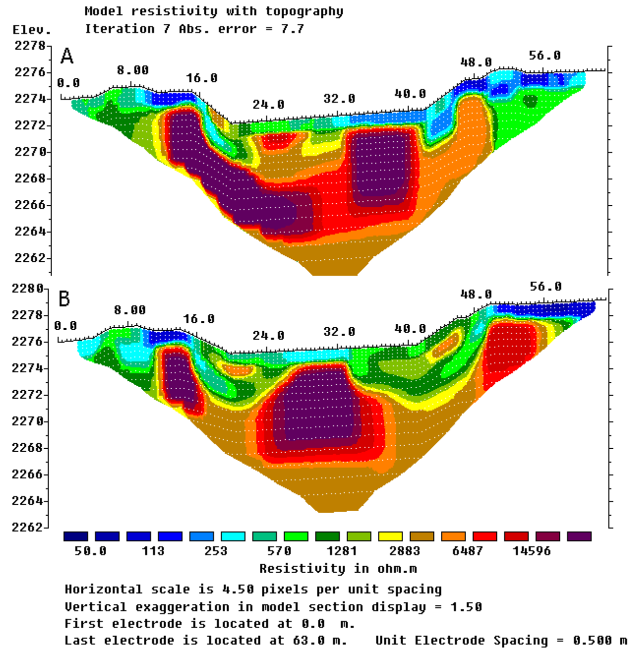

Figure 9. Transverse ERT profiles of the road in section 3 of site 2. The resistivity value is the same as in Figure 3. A-k15-1 profile, B-k15-2 profile

3.2 Ground temperature under the road

In each section, we have installed one monitoring system that records the temperature at the bottom of the evaporator and in the ground under the road between the thermosyphons since December 2022. Also, starting in 2022, the ground temperature under the road is recorded in a section without a thermosyphon. Due to the collapse of the borehole wall, temperature sensors were installed at different depths from the surface.

3.2.1 Section 1 (k13+600:k13+800)

In section 1, to monitor the cooling effect of the thermosyphon, the temperature sensor was installed at a depth of 3.0 m from the road surface on the evaporator pipe, and to control the freezing radius between the thermosyphons, the temperature sensor was installed at a depth of 3.75 m from the road surface.

The thermosyphon operates until early May 2023, and until mid-February 2023, the ground cooled to -14 °C. After this, the ground temperature warmed and rose to -0.4 °C on August 1, 2023. Between thermosyphons, the ground temperature dropped to -8.0 °C until early March 2023 and rose to -2.1 °C in early August 2023 (Figure 10).

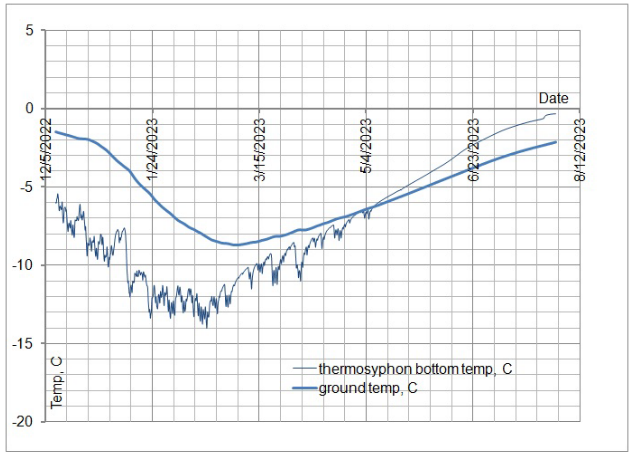

Figure 10. Theromsyphon bottom and ground temperature under the road at section 1, site 2

3.2.2 Section 2 (k14+360:k14+500)

In section 2, to monitor the cooling effect of the thermosyphon, the temperature sensor was installed at a depth of 2.3 m from the road surface on the evaporator pipe, and to control the freezing radius between the thermosyphons, the temperature sensor was installed at a depth of 3.0 m from the road surface.

Thermosyphon's operation period is similar to section 1, and until mid-February 2023, the ground cooled down to -20 °C. After this, the ground temperature warmed and rose to +1.6 °C on August 1, 2023. Between thermosyphons, the ground temperature dropped to -9.0 °C until the end of February 2023 and rose to -0.9 °C in early August 2023 (Figure 11).

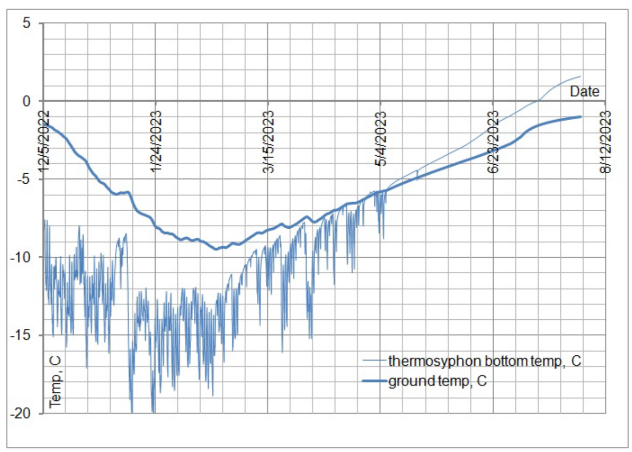

Figure 11. Thermosyphon bottom and ground temperature under the road at section 2, site 2

3.2.3 Section 3 (k15+160:k15+300)

In section 3, to monitor the cooling effect of the thermosyphon, the temperature sensor was installed at a depth of 3.0 m from the road surface on the evaporator pipe, and to control the freezing radius between the thermosyphons, the temperature sensor was installed at a depth of 3.75 m from the road surface.

Thermosyphon's operation period is similar to in section 1, and until mid-February 2023, the ground cooled down to -16 °C. After this, the ground temperature warmed and rose to -0.7 °C on August 1, 2023. Between thermosyphons, the ground temperature dropped to -8.0 °C until the end of February 2023 and rose to -2.2 °C in early August 2023 (Figure 12).

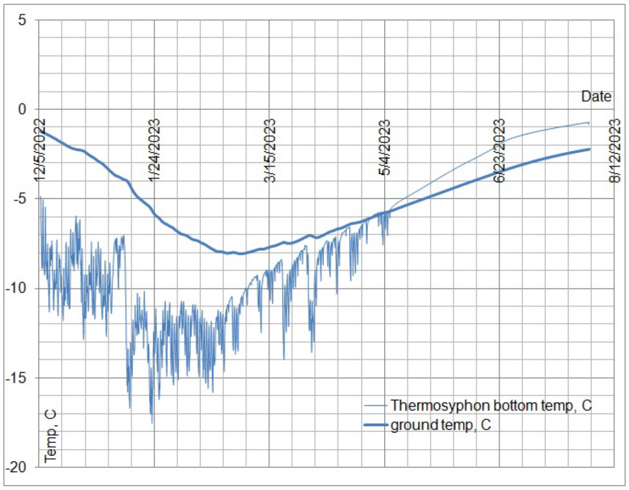

Figure 12. Thermosyphon bottom and ground temperature under the road at section 3, site 2

To compare the soil temperature under a road with and without a thermosyphon, we installed a temperature sensor at a depth of 3.8 m from the road surface on a section of the road without a thermosyphon. By the end of March 2023, the temperature dropped to -3.2 °C. After this, the ground temperature warmed, and on August 1, 2023, it rose to -0.9 °C (Figure 13).

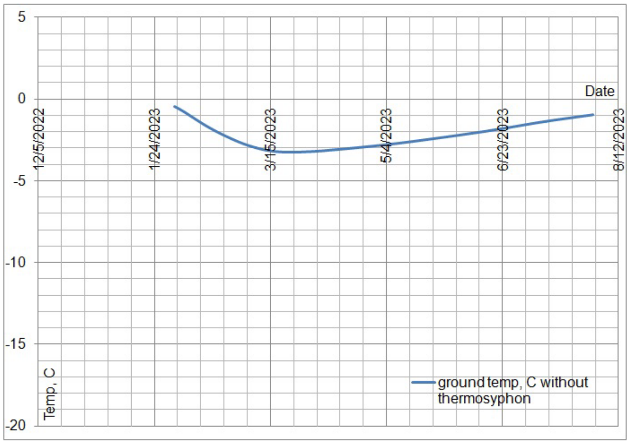

Figure 13. Ground temperature under road without thermosyphon.

4 Discussion

For permafrost studies, ERT surveys were used widely (Lewkowicz et al. 2011; Etzelmuller et al. 2006; Ishikawa et al. 2005, 2001; Hauck et al. 2004), but the use of ERT surveys was relatively less, especially for the study of permafrost under the road (Saruulzaya et al. 2018). Thus, the current study was purposed to investigate the permafrost condition by ERT surveys and monitor the ground temperature under paved roads with thermosyphon and the ground temperature without thermosyphon. The cooling effect of thermosyphon under paved roads was also quantitatively investigated.

4.1 ERT survey

Our ERT profiles showed good contrasts between frozen and unfrozen layers, even in coarse sediments along the road (Figures 5–9). The thickness of the permafrost (approximately 15 m) and the active layer, as well as ice contents, are visible from our ERT profiles. We confirmed them by drilling boreholes in some electrode locations along the ERT lines. For instance, Lewkowicz et al. (2011) and Etzelmuller et al. (2006) suggested that ERT surveys are not a panacea and require additional investigation, such as drilling boreholes, temperature measurement in boreholes, and probing.

The results of ERT surveys indicated that in the upper layer of permafrost, changes begin immediately after the destruction and cutting of the surface layers, and the thawing bowl under the road forms several years later (Jambaljav et al. 2019).

Depending on the ground materials, a thawing bowl forms directly under the road due to the high adsorption of the asphalt pavement and along the sides of the road where the coarse material is located. A thawing bowl forms directly under the road in areas where the ground contains less infiltration material (clay, silt) and directly under the road and along the roadsides where the ground is a good infiltration material (coarse ground). Thus, two distinct thawing events occurred: the first due to increased solar adsorption and the second due to the infiltration and concentration of rain and snowmelt water in the roadside channels.

4.2 Ground temperature

The thermosyphon cools the temperature underground as much as it is cold enough outside.

This finding is supported by several international scholars who indicate the method of cooling the roadbed and thermosyphon cooling, confirmed empirically and by modeling methods (Haynes et al. 1988; Cheng et al. 2006).

Since our monitoring began at the beginning of December 2022, the thermosyphon works to cool the subgrade until the beginning of May 2023. The cooling capacity of a thermosyphon varies along the length of the evaporator pipe. The minimum temperature at the evaporator pipe was -20 °C at 2.3 m from the road surface and -14 °C or -16 °C at a depth of 3.0 m from the road surface. At the end of the summer of 2023, these temperatures were +1.6 °C, -0.9 °C, and -2.1 °C, respectively.

The time shift of temperature fluctuations to a minimum value is half a month for the temperature in the evaporator pipe and between the thermosyphons. Moreover, for the temperature at the evaporator pipe and the temperature without a thermosyphon, this time is 1.5 months.

4.3 Thermal performance of thermosyphon

Thermosyphons can effectively extract heat from the ground without any additional power supply, and they have been widely used to prevent the thawing of permafrost in foundations for many decades (Yarmak et al. 2002; Cheng et al. 2008). They cooled the ground under the infrastructure quite well.

The thermosyphon reduces the ground temperature under the road with a thermosyphon by more than 4 times when comparing the ground temperature under the road without a thermosyphon. The minimum ground temperature was -14 °C or -20 °C under the road with a thermosyphon, and under the road without a thermosyphon, it was -3.2 °C during the monitoring period.

Near site 2, the minimum temperature is -2.45 °C and the maximum is +1.34 °C at a depth of 3 m from the ground surface in the monitoring borehole. Moreover, these temperatures were 5.5 or 6 times colder under paved roads than the temperature from the monitoring borehole at a depth of 3 m. Under a paved road, the maximum temperature is 1.49 times lower than the temperature at a depth of 3 m in the monitoring borehole.

In the warm season, the paved surface heats the underground materials more strongly, and the thermosyphon cools quite well in the cold season.

In Mongolia, the thermosyphon works very well, but installing pretty good insulation above the evaporators under the paved road is necessary.

The present study has limitations. The first limitation is the short monitoring period and air and road surface temperature data, which are limited. However, from 2023, we begin to record these data. Another major limitation is that we focused on construction and monitoring, but we should have considered modeling. We invite anyone to cooperate in modeling thermosyphon cooling for a long period.

5 Conclusions

1. There are two types of permafrost thawing under and along the paved road. Due to increased solar adsorption, a permafrost thawing bowl is formed under a paved road, and due to the accumulation of rain and melted snow water, permafrost thawing is observed on both sides of the road.

2. Thawing of permafrost begins immediately after the destruction or cutting of the earth's surface, and a permafrost thawing bowl forms several years later.

3. Field measurements show that the rate of permafrost thawing under natural conditions is 0.5–2.0 cm per year, and permafrost thawing under paved roads is 5–10 times faster than under natural conditions.

4. The thermosyphon reduces the ground temperature under a paved road with a thermosyphon by more than 4 times compared to a paved road without a thermosyphon.

6 Acknowledgements

The Asian Development Bank financially supported this project under the Western Regional Road Corridor Investment Program (Tranche 2).

We are happy to express our thanks to all of the project participants who worked on this project. Special thanks go to B. Bayan-Amgalan, project coordinator, Ram Prakash, engineer-cum-Team Leader of the Consultant, Ch. Enkhjargal, from an ICT consulting company, and B. Muratbek, from a local road company.

7 References

Cheng, G. 2005. 'A roadbed cooling approach for the construction of Qinghai–Tibet Railway', *Cold Regions Science and Technology* 42(2), pp. 169–176, ISSN 0165-232X. Available at: https://doi.org/10.1016/j.coldregions.2005.01.002.

Guodong Cheng, G., Sun, Z. and Niu, F. 2008. 'Application of the roadbed cooling approach in Qinghai–Tibet railway engineering', *Cold Regions Science and Technology* 53(3), pp. 241–258, ISSN 0165-232X. Available at: https://doi.org/10.1016/j.coldregions.2007.02.006.

Etzelmüller, B., Heggem, E.S.F., Sharkhuu, N., Frauenfelder, R., Kääb, A. and Goulden, C. 2006. 'Mountain permafrost distribution modelling using a multi-criteria approach in the Hövsgöl area, northern Mongolia', *Permafrost and Periglacial Processes* 17(2), pp. 91–104. Available at: https://doi.org/10.1002/ppp.554.

Hauck, C., Isaksen, K., Vonder Mühll, D. and Sollid, J.L. 2004. 'Geophysical surveys designed to delineate the altitudinal limit of mountain permafrost: an example from Jotunheimen, Norway', *Permafrost and Periglacial Processes* 15(3), pp. 191–205. Available at: https://doi.org/10.1002/ppp.493.

Haynes F.D. and Zarling J.P. 1988. 'Thermosyphons and foundation design in cold regions', *Cold Regions Science and Technology*, 15(3), pp. 251–259, ISSN 0165-232X. Available at: https://doi.org/10.1016/0165-232X(88)90072-9.

Ishikawa M, Jamvaljav Y, et al. 2018. 'Thermal states, responsiveness and degradation of marginal permafrost in Mongolia', *Permafrost and Periglacial Processes* 29(4), pp. 271–282. Available at: https://doi.org/10.1002/ppp.1990.

Ishikawa, M., Sharkhuu, N., Zhang, Y., Kadota, T. and Ohata, T. 2005. 'Ground thermal and moisture conditions at the southern boundary of discontinuous permafrost, Mongolia', *Permafrost and Periglacial Processes* 16(2), pp. 209–216. Available at: https://doi.org/10.1002/ppp.483.

Ishikawa, M. and Hirakawa, K. 2000. ‘Mountain permafrost distribution based on BTS measurements and DC resistivity soundings in the Daisetsu Mountains, Hokkaido, Japan’, *Permafrost and Periglacial Processes* 11(2), pp. 109–123. Available at: https://doi.org/10.1002/1099-1530(200004/06)11:2<109::AID-PPP343>3.0.CO;2-O.

Jambaljav, Y. 2017. *Permafrost distribution and changes over Mongolia*. Ulaanbaatar, Mongolia: Colorful Ochir Press. ISBN 978-99978-1-862-1. 78 p. (in Mongolian).

Jambaljav, Y., Saruulzaya, A., et al. 2013. *Establishment of permafrost monitoring network over Mongolia*. Ulaanbaatar, Mongolia: Scientific report of the project funded by Mongolian Science and Technology (in Mongolian).

Jambaljav, Y., Saruulzaya, A., Tsogt-Erdene, et al. 2019. *Permafrost study along some road*. Ulaanbaatar, Mongolia: Scientific report of the project funded by Mongolian Science and Technology (in Mongolian).

Lewkowicz, A.G., Etzelmüller, B. and Smith, S.L. 2011. ‘Characteristics of Discontinuous Permafrost based on Ground Temperature Measurements and Electrical Resistivity Tomography, Southern Yukon, Canada’, Permafrost Periglacial and Processes 22(4), pp. 320–342. Available at: https://doi.org/10.1002/ppp.703.

Loke, Meng 2001. *Tutorial: 2-D and 3-D Electrical Imaging Surveys*. Available at: www.geoelectrical.com.

Saruulzaya, A., Jambaljav, Y., Gansukh, Y., et al. 2018. ‘High-resolution Electrical Resistivity Tomography (ERT) measurements along the paved roads in permafrost regions of Mongolia’, in *5th European Conference on Permafrost*, Universite Savoie Mont Blanc, Chamonix, France, 23 June–1 July, 2018.

Sharkhuu, N. and Anarmaa, S. 2011. ‘Long-term monitoring of permafrost in Mongolia’, in *Extended abstracts of international second symposium on mountain and arid land permafrost*, OOP LLC, Ulaanbaatar, Mongolia, pp. 59–61.

Ministry of Road and Transport Development 2022. *Statistical data of Mongolia for 2022*. Available at: mrtd.gov.mn.

Yamkhin, J., Yadamsuren, G., Khurelbaatar, T., et al. 2022. ‘Spatial distribution mapping of permafrost in Mongolia using TTOP’, *Permafrost and Periglacial Processes* 33(4), pp. 386–405. doi:10.1002/ppp.2165.

Yarmak, E., Jr. and Long, E.L. 2002. ‘Recent developments in thermosyphon technology’, in K.S. Merrill (ed.), *Proceedings of the 11th International Conference on Cold Regions Engineering*. Anchorage, Alaska, United States. pp. 656–662.